Journal of Solid State Chemistry 182 (2009) 3383–3386

Contents lists available at ScienceDirect

Journal of Solid State Chemistry

journal homepage: www.elsevier.com/locate/jssc

Facile synthesis of PbTe nanoparticles and thin films in alkaline aqueous solution at room temperature

Y.Y. Wang, K.F. Cai *, X. Yao

Tongji University, Functional Materials Research Laboratory, 1239 Siping Road, Shanghai 200092, China

ARTICLE INFO

Article history:
Received 9 July 2009
Received in revised form
30 September 2009
Accepted 5 October 2009
Available online 14 October 2009

Keywords:
PbTe
Film
Nanoparticle
Thermoelectric properties
Chemical bath deposition

ABSTRACT

A novel, simple, and cost-effective route to PbTe nanoparticles and films is reported in this paper. The PbTe nanoparticles and films are fabricated by a chemical bath method, at room temperature and ambient pressure, using conventional chemicals as starting materials. The average grain size of the nanoparticles collected at the bottom of the bath is ~25 nm. The film deposited on glass substrate is dense, smooth, and uniform with silver gray metallic luster. The film exhibits p-type conduction and has a moderate Seebeck coefficient value (~147 $\mu V K^{-1}$) and low electrical conductivity (~0.017 $S cm^{-1}$). The formation mechanism of the PbTe nanoparticles and films is proposed.

1. Introduction

Lead telluride (PbTe) is a narrow band gap (E_g=0.32 eV) semiconductor. It has been reported that PbTe and PbTe based materials have superior thermoelectric (TE) properties [1,2] and have potential applications in power generation and thermal sensing. Theoretical calculations and experiments indicate that improvement in TE properties can be achieved as the dimensionality of materials is reduced [1,3–7]. Low dimensional TE materials such as films are of great interest for construction of high performance TE devices. In addition, PbTe films are also good candidates for optoelectronic applications in the mid-infrared range [8].

Various methods have been utilized to prepare PbTe thin films, such as vacuum evaporation [9–12], magnetron sputtering [13], molecular beam epitaxy [14], pulsed laser deposition [15], hot-wall epitaxy [16,17], and electrodeposition [18–20]. All these methods need special equipments, and the electrodeposition method needs conductive substrates, although it is relatively low-cost. Chemical bath deposition (CBD) method does not have special requirement for substrate and does not need special equipment, therefore, it is much more convenient and more cost-effective. Lead chalcogenide thin films prepared by CBD method have recently been reported. For example, PbS thin films were deposited on glass or Si substrates using thiourea or sodium thiosulfate as the S source [21–24]; PbSe films were deposited on glass substrate, using sodium selenosulfate (Na_2SeSO_3) as the Se source [25,26]. Unfortunately, the corresponding Te source, Na_2TeSO_3, is hard to obtain and instable. Moreover, the hydrolysis and disproportionating reaction of Te in solution is much more difficult than those of S or Se [27]. Therefore, there are rare studies on deposition of PbTe thin films by CBD method.

In this work, we report for the first time on PbTe thin film deposited on glass substrate and the synthesis of PbTe nanoparticles, at room temperature, in an alkaline aqueous solution, by a CBD method. The present method for preparation of PbTe film is much simpler and cost effective than the other methods mentioned above. On the other hand, compared with other methods, such as solvothermal/hydrothermal synthesis methods [28–30], high temperature solution-phase synthesis [31] and sonoelectrochemical approach [32], for synthesis of PbTe nanoparticles, our present method is much more convenient. The formation mechanism of the PbTe nanoparticles and film was proposed and the TE properties of the film were measured at room temperature.

2. Experimental procedures

All reagents were analytical grade and directly used without further purification. In a typical run, 1 mmol $Pb(Ac)_2 \cdot 3H_2O$, 1 mmol TeO_2, 0.02 mol KOH, 2 mmol trisodium citrate (TSC), and 8 mmol KBH_4 were dissolved in sequence in 50 ml deionized water. A colorless and transparent solution was formed. The solution was diluted to 200 ml in a beaker and then was placed at

* Corresponding author. Fax: +86 21 65980255.
E-mail addresses: kfcai@mail.tongji.edu.cn, kfcai@tongji.edu.cn (K.F. Cai).

0022-4596/$ - see front matter © 2009 Elsevier Inc. All rights reserved.
doi:10.1016/j.jssc.2009.10.004

room temperature without stirring. Microscope glass slide was used as the substrate after being ultrasonically cleaned in pure ethanol for 15 min and then rinsed with deionized water. The slide was put in the solution at an angle of ~30° to the bottom of the beaker. The solution gradually turned dark. About 12 h later, the solution was in black and films with silver gray metallic luster (see supporting data SD1) were formed on both sides of the substrate and inwall of the beaker immerged in the solution. The film deposited on the downward side of the substrate was more strongly adhered while that on the upward side was weakly adhered and could be removed with a cotton swab wetted by oxalic acid solution (0.1 mol L^{-1}). Therefore, hereinafter, only the film deposited on the downward side of the substrate was further studied. Black precipitate was collected at the bottom of the beaker about 24 h later. The precipitate was washed with deionized water and pure ethanol in sequence for several times, then separated by centrifugation for 5 min at 4000 rpm and finally dried in vacuum at 70 °C.

The phase composition of the precipitate and the film was determined by X-ray diffraction (XRD, Bruker D8 Advanced) with Cu$K\alpha$ radiation (λ=1.5406 Å). The morphology and composition of the precipitate were examined by transmission electron microscopy (TEM, Philips TECNAI-20), equipped with an energy dispersive X-ray spectroscopy (EDS). The morphology of the film was observed by field emission scanning electron microscopy (FE-SEM, Quanta 200 FEG). The electrical conductivity and Seebeck coefficient of the film were measured at room temperature. A standard four-probe method was used for the electrical conductivity measurement and the Seebeck coefficient was determined by the slope of the linear relationship between the thermoelectromotive force and temperature difference (~10 K) between two points on the film.

3. Results and discussion

Figs. 1(a) and (b) show typical XRD patterns for the precipitate and the film, respectively. All the diffraction peaks for the precipitate can be indexed to the reported PbTe (JCPDS card file, No. 077–0246), indicating that the precipitate is PbTe. The average particle size of the precipitate is estimated to be about 21 nm from the Scherrer formula: $d=k\lambda/w\cos\theta$, where d is the particle size, k is the Scherrer constant (0.9) and w is the half width of the diffraction peak. For the film, its XRD pattern only has three weak peaks at 2θ= ~27.5, 39.3, and 64.4° with a hillside background. The three weak peaks can also be indexed to the PbTe (JCPDS card file, No. 077–0246), and the hillside background should be due to the glass substrate. This indicates that the film also consists of PbTe.

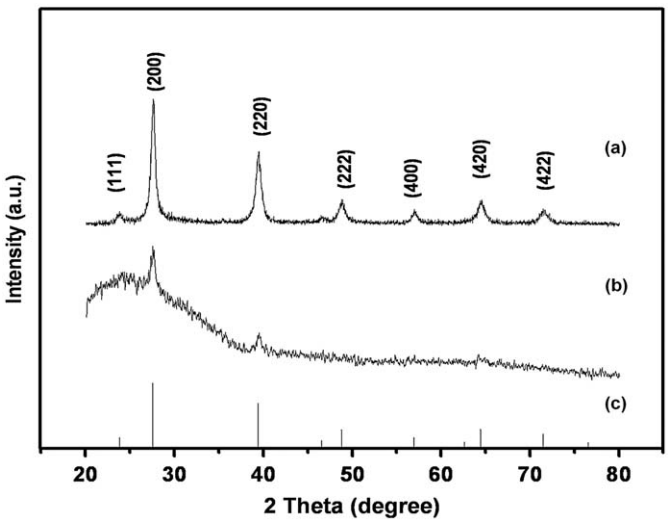

Fig. 1. Typical XRD patterns of (a) precipitate, (b) film, and (c) the standard pattern of PbTe (JCPDS card file, no. 077-0246), respectively.

Fig. 2(a) shows a typical TEM image of the precipitate. It can be seen from Fig. 2(a) that the precipitate is uniform and consists of nanoparticles with average particle size of ~25 nm, which is close to the calculated size from XRD data. EDS analysis indicates that the nanoparticles are composed of Pb and Te (see Fig. 2(b)), and that the atomic ratio of Pb/Te is very close to 1:1, which further confirms that the precipitate is PbTe. The Cu signals in Fig. 2(b) should be from the copper grid of the TEM sample holder.

Figs. 3(a) and (b) are typical FE-SEM images of the surface morphology of the film at low and high magnification, respectively. It can be seen from Figs. 3(a) and (b) that the PbTe film is dense and homogeneous. The film surface consists of numerous nanoparticles, and the exact sizes of the nanoparticles are difficult to be determined due to agglomeration. The thickness of the film is about 1 μm estimated from its fracture section under SEM (see supporting data SD2).

Two additional experiments (experiments A and B) were performed to explore the formation mechanism of the PbTe. The experiment A and B were done under the same conditions as described above but without adding $Pb(Ac)_2\cdot 3H_2O$ and using Te powder instead of TeO_2, respectively. For experiment A, only a little black precipitate was formed at the bottom of the beaker and no films were deposited. The precipitate was elemental Te determined by means of XRD. For experiment B, the whole system was hardly changed during the reaction time as the Te powder cannot be well dissolved by alkaline solution at room temperature. The experiment A indicates that at room temperature the TeO_2 can be reduced to Te by KBH_4 but can not be reduced to Te^{2-}, while the experiment B indicates that the Pb^{2+} from $Pb(Ac)_2$ cannot be reduced into Pb in the system. Based on the above results, the whole reaction process for the formation of the PbTe was proposed as follows:

$$Pb^{2+}+3OH^- \Rightarrow HPbO_2^-+H_2O \quad (1)$$

$$TeO_2+2OH^- \Rightarrow TeO_3^{2-}+H_2O \quad (2)$$

$$HPbO_2^-+H_2O \Rightarrow Pb^{2+}+3OH^- \quad (3)$$

$$Pb^{2+}+TeO_3^{2-} \Leftrightarrow PbTeO_3 \quad (4)$$

$$2PbTeO_3+6BH_4^- \Rightarrow 2PbTe+6OH^-+3B_2H_6\uparrow \quad (5)$$

The $Pb(Ac)_2$ and TeO_2 dissolve in excess alkali and form $HPbO_2^-$ and TeO_3^{2-} ions, according to reactions (1) and (2), respectively. The TeO_3^{2-}, $HPbO_2^-$ and BH_4^- (from KBH_4) all are negative charges; therefore, the reduction reactions related to them are difficult. Some $HPbO_2^-$ ions are hydrolyzed into Pb^{2+} (reaction (3)). The Pb^{2+} combines with the TeO_3^{2-} to form $PbTeO_3$ colloidal particles (reaction (4)). The $PbTeO_3$ colloidal particles are reduced into PbTe by BH_4^- (reaction (5)) and PbTe nuclei form. The PbTe nuclei attached to the surface of the substrate and the inwall of the beaker grow up and form films, and the PbTe nuclei in the solution grow up slowly into nanoparticles and precipitate at the bottom of the beaker. The deposition procedure was carried out at room temperature, therefore, the growth of the PbTe nuclei should be very slow and the products consist of nanoparticles.

The TSC was used as a complexing agent [25]. The films deposited without adding TSC were loose and easy to peel off, indicating that the TSC can increase the adhesive ability of the films. However, when the TSC concentration was increased to

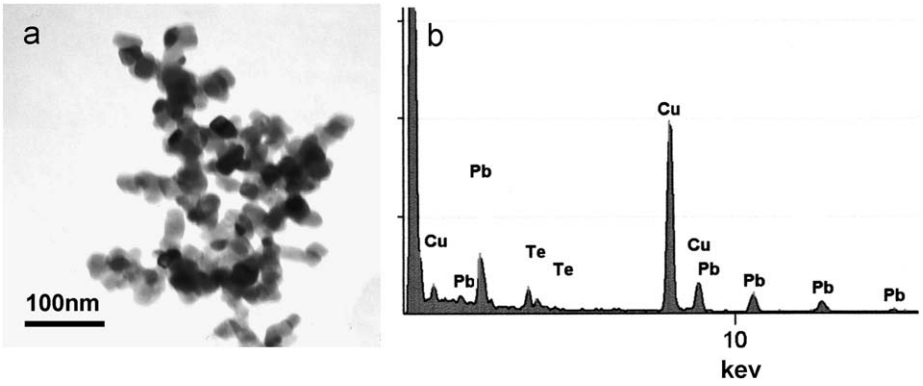

Fig. 2. Typical TEM image (a) and EDS spectrum (b) of the precipitate

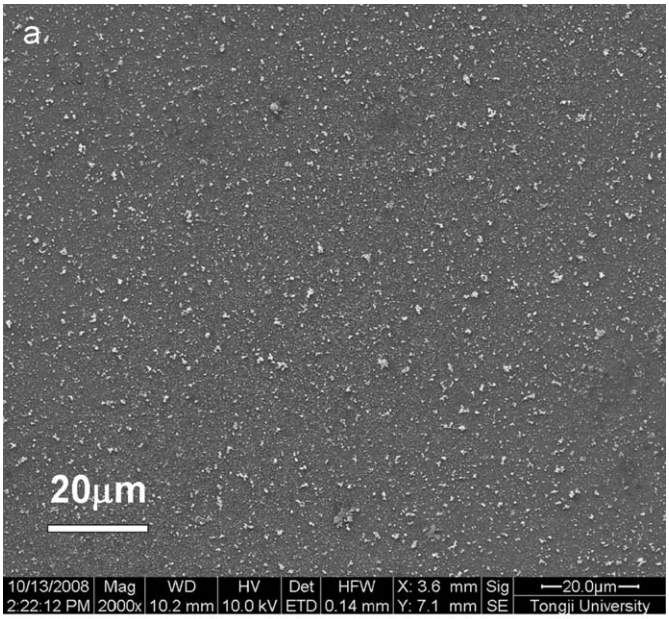

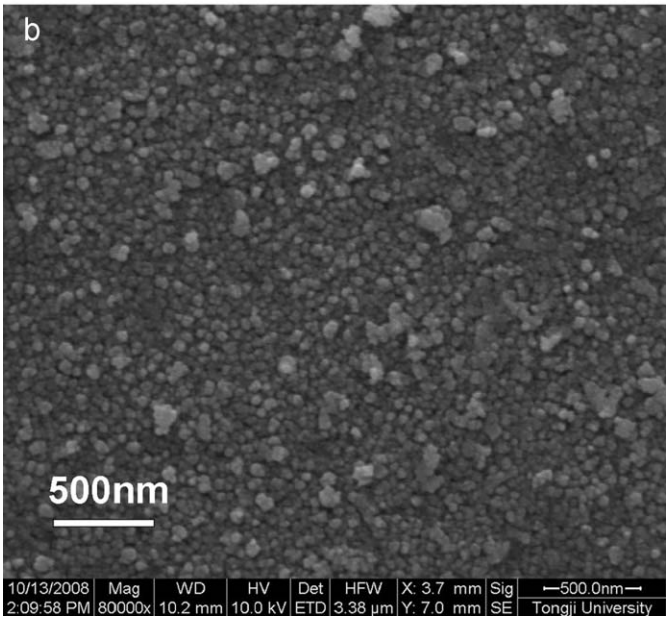

Fig. 3. Typical FE-SEM images of the surface morphology of the film deposited on glass substrate at (a) low and (b) high magnification.

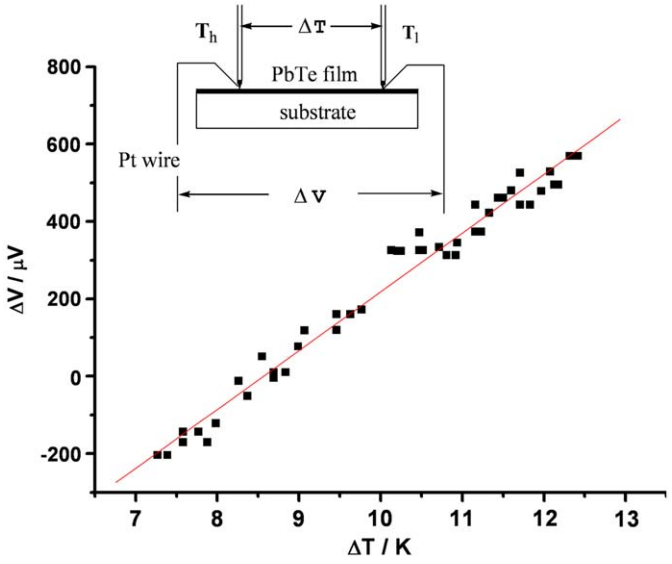

Fig. 4. Plot of thermoelectromotive force versus temperature difference from two points on the film, inset is a schematic diagram of the Seebeck coefficient measurement.

0.02, 0.04 or 0.1 mol L^{-1}, the films formed were quite similar. The influence of the KOH concentration was also investigated. When the KOH concentration was too low (~0.01 mol L^{-1}), PbTe nanoparticles precipitated quickly but no films were formed. When the KOH concentration was too high (~1 mol L^{-1}), the solution was very stable and even 72 h later neither PbTe films nor nanoparticles were formed.

The electrical conductivity (σ) and Seebeck coefficient (S) of the film are ~0.017 S cm^{-1} and ~147 μV K^{-1} (see plot of thermoelectromotive force versus temperature difference from two points on the film in Fig. 4), indicating that the film is p-type conductor. Both the values of electrical conductivity and Seebeck coefficient are lower than those of the PbTe films (~0.28–1.12 S cm^{-1} and ~200–400 μV K^{-1}, at room temperature) prepared by a gas evaporation method [12]. The low electrical conductivity of the film should be due to a strong grain boundaries scattering of carriers. Nevertheless, extremely low thermal conductivity (κ) for the film could be expected due to strong grain boundaries scattering to the phonons. This is beneficial to the nondimensional TE figure of merit, ZT ($=\sigma S^2 T/\kappa$, where T is the absolute temperature), which determines the TE conversion efficiency of a material. The TE properties of the film

could be improved by doping other elements, such as Ag, Sb, Sn, and Se.

4. Conclusions

A novel, simple, convenient, and low-cost route to PbTe nanoparticles and films is presented. PbTe film with silver gray metallic luster is successfully deposited on glass substrate at room temperature and ambient pressure. The film is dense, smooth, and uniform. The electrical conductivity and Seebeck coefficient of the film are $\sim 0.017\,S\,cm^{-1}$ and $\sim 147\,\mu V\,K^{-1}$, respectively. The PbTe nanoparticles collected at the bottom of the bath are homogeneous and with grain size of ~ 25 nm.

As the processing is very simple, the reaction condition is very mild, and no special equipment is needed, this route to PbTe nanoparticles and films shall be very promising.

Acknowledgments

This work was supported by National Natural Science Foundation of China (50872095) and the 973-project under Grant no. 2007CB607500. The authors thank Prof. J.Y. Yang from Huazhong University of Science and Technology, China, for measuring the thermoelectric properties.

Appendix A. Supplementary material

Supplementary data associated with this article can be found in the online version at 10.1016/j.jssc.2009.10.004.

References

[1] T.C. Harman, P.J. Taylor, M.P. Walsh, B.E. LaForge, Science 297 (2002) 2229.
[2] K.F. Hsu, S. Loo, F. Guo, W. Chen, J.S. Dyck, C. Uher, T. Hogan, E.K. Polychroniadis, M.G. Kanatzidis, Science 303 (2004) 818.
[3] L.D. Hicks, T.C. Harman, X. Sun, M.S. Dresselhaus, Phys. Rev. B 53 (1996) 10493.
[4] T.C. Harman, P.J. Taylor, D.L. Spears, M.P. Walsh, J. Electron. Mater. 29 (2000) L1.
[5] L.D. Hicks, M.S. Dresselhaus, Phys. Rev. B 47 (1993) 12727.
[6] P.F.R. Poudeu, J. D'Angelo, A.D. Downey, J.L. Short, T.P. Hogan, M.G. Kanatzidis, Angew. Chem. Int. Ed. 45 (2006) 3835.
[7] J.R. Sootsman, H. Kong, C. Uher, J.J. D'Angelo, C.I. Wu, T.P. Hogan, T. Caillat, M.G. Kanatzidis, Angew. Chem. Int. Ed. 47 (2008) 8618.
[8] S.S. Sahay, S. Guruswamy, J. Mater. Sci. Lett. 17 (1998) 1145.
[9] T. Komissarova, D. Khokhlov, L. Ryabova, Z. Dashevsky, V. Kasiyan, Phys. Rev. B 75 (2007) 195326.
[10] E.I. Rogacheva, I.M. Krivulkin, O.N. Nashchekina, A.Y. Sipatov, V.V. Volobuev, M.S. Dresselhaus, Appl. Phys. Lett. 78 (2001) 1661.
[11] E.I. Rogacheva, T.V. Tavrina, O.N. Nashchekina, V.V. Volobuev, A.G. Fedorov, A.Y. Sipatov, M.S. Dresselhaus, Thin Solid Films 423 (2003) 257.
[12] M. Ito, W.S. Seo, K. Koumoto, J. Mater. Res. 14 (1999) 209.
[13] A. Jdanov, J. Pelleg, Z. Dashevsky, R. Shneck, Mater. Sci. Eng. B—Solid State Mater. Adv. Technol. 106 (2004) 89.
[14] H. Zogg, K. Alchalabi, D. Zimin, Defence Sci. J. 51 (2001) 53.
[15] A. Jacquot, B. Lenoir, M.O. Boffoue, A. Dauscher, Appl. Phys. A—Mater. Sci. Process. 69 (1999) S613.
[16] M.K. Sharov, Y.A. Ugai, J. Surf. Invest. 2 (2008) 481.
[17] H.Y. Chen, S.S. Dong, Y.K. Yang, D.M. Li, J.H. Zhang, X.J. Wang, S.H. Kan, G.T. Zou, J. Cryst. Growth 273 (2004) 156.
[18] H. Saloniemi, T. Kanniainen, M. Ritala, M. Leskela, Thin Solid Films 326 (1998) 78.
[19] F. Xiao, B. Yoo, M.A. Ryan, K.H. Lee, N.V. Myung, Electrochim. Acta 52 (2006) 1101.
[20] X.H. Li, I.S. Nandhakumar, Electrochem. Commun. 10 (2008) 363.
[21] I. Pop, C. Nascu, V. Ionescu, E. Indrea, I. Bratu, Thin Solid Films 307 (1997) 240.
[22] A.A. Rempel, N.S. Kozhevnikova, A.J.G. Leenaers, S. van den Berghe, J. Cryst. Growth 280 (2005) 300.
[23] M.S. Ghamsari, M.K. Araghi, S.J. Farahani, Mater. Sci. Eng. B—Solid State Mater. Adv. Technol. 133 (2006) 113.
[24] Y.J. Yang, S.S. Hu, Thin Solid Films 516 (2008) 6048.
[25] S. Gorer, A. Albuyaron, G. Hodes, Chem. Mater. 7 (1995) 1243.
[26] S. Gorer, A. Albuyaron, G. Hodes, J. Phys. Chem. 99 (1995) 16442.
[27] W.X. Zhang, Z.H. Yang, J.W. Liu, Y.T. Qian, W.C. Yu, Y.B. Jia, X.M. Liu, G. Zhou, J.S. Zhu, J. Solid State Chem. 161 (2001) 184.
[28] H. Li, K.F. Cai, H.F. Wang, L. Wang, J.L. Yin, C.W. Zhou, J. Solid State Chem. 182 (2009) 869.
[29] W.Z. Wang, B. Poudel, D.Z. Wang, Z.F. Ren, Adv. Mater. 17 (2005) 2110.
[30] G. Zhang, X. Lu, W. Wang, X. Li, Chem. Mater. 19 (2007) 5207.
[31] J.E. Murphy, M.C. Beard, A.G. Norman, S.P. Ahrenkiel, J.C. Johnson, P.R. Yu, O.I. Micic, R.J. Ellingson, A.J. Nozik, J. Am. Chem. Soc. 128 (2006) 3241.
[32] X.F. Qiu, Y.B. Lou, A.C.S. Samia, A. Devadoss, J.D. Burgess, S. Dayal, C. Burda, Angew. Chem. Int. Ed. 44 (2005) 5855.